4-1-2013

Explaining the Hydroclimatic Variability and Change in the Salmon River Basin

Venkataramana Sridhar
Boise State University

Xin Jin
Boise State University

W. Thilini Jaksa
Boise State University

 DOI: 10.1007/s00382-012-1467-0

Explaining the Hydroclimatic Variability and Change in the Salmon River Basin

V. Sridhar, Xin Jin, and W. T. Jaksa

Department of Civil Engineering
Boise State University

Summary

Climate change in the Pacific Northwest and in particular, the Salmon River Basin (SRB), is expected to bring about 3 -5 °C rise in temperatures and an 8% increase in precipitation. In order to assess the impacts due to these changes at the basin scale, this study employed an improved version of Variable Infiltration Capacity (VIC) model, which includes a parallel version of VIC combined with a comprehensive parameter estimation technique, Shuffled Complex Evolution (SCE) to estimate the streamflow and other water balance components. Our calibration (1955-75) and validation (1976-99) of the model at the outlet of the basin, White Bird, resulted in an r^2 value of 0.94 which was considered satisfactory. Subsequent center of timing analysis showed that a gradual advancement of snowmelt induced-peak flow advancing by about 10 days in the future. Historically, the flows have shown a general decline in the basin, and in the future while the magnitudes might not be greatly affected, decreasing runoff of about 3 % over the next 90 years could be expected and timing of peak flow would shift by approximately 10 days. Also, a significant reduction of snow water equivalent up to 25%, increased evapotranspiration up to 14%, and decreased soil moisture storages of about 2 % is predicted by the model. A steady decline in SWE/P from the majority of climate model projections for the basin was also evident. Thus, the earlier snowmelt, decreasing soil moisture and increased evapotranspiration collectively implied the potential to trigger drought in the basin and could affect the quality of aquatic habitats and their spawning and a detailed investigation on these impacts is warranted.

Keywords: Hydrologic Impacts, Climate Change, VIC modeling, Parameter estimation, Salmon River

1. Introduction

Many river basins in the Pacific Northwest including the Salmon River Basin (SRB), is experiencing hydrologic changes over the past several decades, possibly due to climate change and climate variability (Barnett et al. 2005; Hamlet et al. 2007; Hoekema and Sridhar 2011; Matter et al. 2010; Sridhar and Nayak 2010; Cuo et al., 2011). Changes in temperature and precipitation regimes over the Pacific Northwest , as predicted by the climate models, suggest that a general warming conditions in the future and a range of precipitation scenarios (Mote and Salathe 2010; Abatzoglu, 2011). These projected changes are expected to impact hydrological changes and flow in the river system (Jin and Sridhar 2012; Jung and Chang, 2011a; Jung and Chang, 2011b; Hamlet, 2011). Winter mountain snowpack is the dominant source of streamflow in SRB, however, spatial variability arising out of complex terrain features, including vegetation and distribution of snow controls the streamflow pattern. Accuracy of predicting streamflows becomes important for this natural basin as it provides a best opportunity to evaluate the system wherein any changes in hydrologic conditions, devoid of human-impacts, can be solely attributed to climate change and variability. As the principle of stationarity is increasingly debated (Milly et al. 2008; Jung et al., 2011), understanding of hydroclimatic variability also presents a case to develop plans for ecosystem management and adaptation in the event of abrupt changes induced by the climate system.

In order to understand the climate impacts at the local or regional level, modeling the hydrological processes is a common practice, supported by observations such as streamflow, soil moisture and evapotranspiration. Generally climate models address the land surface part of the water balance reasonably well, however, lacks detail on the spatio-temporal pattern needed for planning and management of water resources at the local scale (Graham et al. 2007a; Kerr 2011). Apart from using regional climate models for impact assessment, one of the common approaches is to force the hydrology or any other impact models such as a crop or ecology model with downscaled climate model outputs (Fowler et al. 2007; Graham et al. 2007a; Graham et al. 2007b; Jin and Sridhar 2012; Olesen et al. 2007) to simulate the basin's hydrological characteristics including streamflow. Macroscale hydrology models that represent the region or the river basin can be a good tool to inform us on the response of the watershed to any changes. The Variable Infiltration Capacity (VIC) macroscale land surface model (Cherkauer et al. 2003; Liang et al. 1994;) has been extensively used in simulating the hydrology of the western U.S. watersheds (Adam et al. 2009; Voisin et al. 2010; Wood et al. 2004; Shukla et al., 2011).

Although SRB has been part of many earlier studies, as a tributary to the Columbia River basin in the Pacific Northwest region, little information exist on the sub-basin heterogeneity in quantifying the streamflow as it is closely related to the amount and timing of precipitation, terrain, wilderness and its impact on the distribution and melting of snow, stream geomorphology and stream temperature. Shi et al. (2008) suggest that hydrologic model calibration is important, however, post-processing of the outputs to correct the bias from the model estimates might be equally valuable. In a gauged basin, using the observed streamflow, parameters that define the streamflow generation are generally calibrated. However, depending on the complexity of the model, parameter estimation can be tedious and often times introduce uncertainties in the estimates of streamflow or the other components of hydrologic cycle. Furthermore, this depends on the quality of observations to perform the bias-correction and density of gauging locations within a watershed. Nonetheless, a well-calibrated hydrology model representing the basin attributes more closely that can reliably predict flows altered by both natural climate variability and climate change is essential to obtain vital details more confidently. Unless the nature and pattern of flows for current and future climatic conditions, both in terms of short and long-term are well-understood, impact assessment and adaptation planning in the face of anticipated hydrologic shifts in flows on the critical issue of salmon migration for spawning and reproduction in the pristine upstream river segments remain a major challenge.

This paper presents the hydrological response of SRB in terms of streamflow scenarios and associated uncertainties involved in understanding the projected impacts of climate change. By estimating the parameters from the automated streamflow calibration exercise at the outlet of the basin, given the lack of field observations from large river basins such as the SRB, our goal is to analyze the range of temperature and precipitation trends from climate models and evaluate their impacts on the basin's water balance and the timing of stream flow. Evaluating alterations to flow regimes is especially important in this vastly undisturbed river basin to maintain the ecosystem integrity and aquatic species' habitats. An automated calibration technique, Shuffled Complex Evolution (SCE) algorithm, coupled with the model will aid in extending this approach to other basins or sub-basins easily. Therefore, our efforts in this study were directed at demonstrating the application of an integrated model that is computationally demanding with a parallel-version of VIC. This study employed an ensemble of GCM-downscaled outputs for the

periods 2010-2100 to evaluate the climate impacts. However, as a prerequisite to this step, this paper tested the calibration scheme incorporated with the model for the period between 1955-1975, and validated for the historic periods, 1976-1999, to characterize the sub-basin processes in SRB.

2. Study Area: River Basin Physiography and Climate

The Salmon River originates in the central and eastern mountains of Idaho and drains an area of about 36,520 km^2 (Figure 1). This river flows north initially and turns west near Salmon, Idaho to join the Snake River near Lewiston, Idaho. Also, nicknamed as the River of No Return, it is about 684 km long and flows through the rugged mountains and diverse vegetation and topographic settings. This is mostly an unmanaged basin in the region with most of the snowmelt from higher elevations at the headwaters flows down the river until it joins with the Snake River with little or insignificant diversions. Since it is mostly a pristine watershed and because of its rich habitats for salmon spawning and its natural course of the river through the rugged mountains it very attractive destination for recreational activities. In particular, the middle fork of the Salmon River is popular for rafting and kayaking. The geographical extent of the basin is between 43° 50' and 46° latitude and 113° 00' and 117°00' longitude, and it comes under the Northern Rocky Mountain Ecoregion. Vegetation in the basin is varied, with sagebrush (*Artemisia*) on the dry south and west facing slopes and Douglas fir (*Pseudotsuga menziesii*) on the wet north and east slopes of the upper basin. Other types of cover include aspen (*Populus tremuloides*), maple (*Acer glabrum*) and meadows in the upper reaches and Ponderosa Pine (*Pinus ponderosa*), black cottonwood (*Populus trichocarpa*) in the lower reaches of the basin (Minshall et al. 1992). While there is distinguishable spatial heterogeneity in terms of vegetation, the main land use categories in the area are forestry, grazing and recreation. Mean annual temperatures range between 4-11 °C depending on the elevation and about 50% of precipitation falls as snow between October and March. Snow depths ranging from 300 cm at the higher elevations to 50 cm at the lower elevations and precipitation between 18 and 38 cm across the basin is typical (Minshall et al. 1992). However, anticipated changes in temperature and precipitation under a warming climate provide a slightly different scenario over the basin which will be discussed in the later sections.

3. Methods

3.1 Variable Infiltration Capacity Model

In order to assess the climate change impacts, we linked the climate model outputs with the VIC model in this study. VIC is a macro-scale, grid-based model representing the soil, vegetation and hydrometeorological conditions of the landscape to simulate exchanges of flux between the surface, sub-surface and atmosphere (Liang et al. 1994, 1996). Numerous studies have implemented the VIC model, ranging from local, river basin, continental and global scales (Abdulla and Lettenmaier 1997; Adam et al. 2009; Nijssen et al. 1997; Maurer et al., 2002). It is a well-documented and validated model. However, the calibration procedure followed by these previous studies was a regular, manual method of identifying the parameters and estimating them based on the observed streamflow available from a known location. There are about 10 parameters representing mostly the soil characteristics (Table 2). Forcing inputs were daily precipitation, maximum and minimum temperature, and daily average wind speed and dew point. Daily gridded meteorological data obtained from the Surface Water Modeling group at the University of Washington from their web site at http://www.hydro.washington.edu/Lettenmaier/Data/gridded/, the development of which is described by Maurer et al. (2002). Briefly describing the methods here, based on station-observed precipitation and temperature, Maurer et al., (2002) generated other variables using empirical relationships derived by others. For example, dew point temperature was derived based on Kimball et al., (1997), shortwave radiation from Thornton and Running (1999), daily 10-m windfields from NCEP-NCAR reanalysis (Kalnay et al., 1996). Maurer et al., (2002) used the synergraphic mapping system (SYMAP) algorithm of Shepard (1984) as implemented by Widmann and Bretherton (2000) to generate the gridded daily precipitation data. Adopting the parameter-elevation regressions on independent slopes model (PRISM) precipitation climatology from Daly et al. (1994; 1997) that is developed statistically to capture local variations of complex terrain, this gridded data were scaled by Maurer et al., (2002) to match this longterm average dataset of 12 monthly means for 1961–90. For future projections, we used the GCM climate model data downloaded from http://gdo-dcp.ucllnl.org/downscaled_cmip3_projections/. Since this downloaded data was from the monthly timestep climate model outputs at a relatively coarser scale (large than 1/8°), an intermediate step of downscaling them was performed, both spatially to 1/8 ° and temporally to daily in order to

link these variables with VIC. We used the delta method of downscaling and the procedures followed are available in Jin and Sridhar (2012). As the first step, a historical year was randomly picked to compute the mean of the daily precipitation and temperature from the gridded observed record for the same month as that of the future year; secondly, the difference between the future monthly mean temperature and the historical mean of the monthly mean temperature, ''□t'' was calculated; followed by this, the ratio between the future monthly mean precipitation and the historical mean of monthly mean precipitation, ''r'' was computed; subsequently, we added ''□t'' to daily temperature of the month of a randomly selected year; multiplied daily precipitation by ''r'' for the month of a randomly selected year; this procedure was repeated for other months of the year for future years and for every grid cell in the study area.

3.2 Calibration using the Shuffled Complex Evolution Technique

We used the Shuffled Complex Evolution (SCE) global optimization technique for calibration of the basin parameters. This is based on upon the procedure described by Duan et al. (1993). The following steps were followed. 1) An initial population of sample points, based on a set of parameter values within their respective ranges, was generated by choosing random parameter values. Objective function (Root Mean Squared Error, RMSE) values were computed for each point. Using default SCE values to calibrate the seven parameters, the initial population would contain 75 samples; 2) The points were sorted by an objective function value. Groups or complexes were created from the population by systematically picking samples from the sorted population. By default, five complexes were created. Each complex was evolved a specified number of times, independently from other complexes and, that number was the same as the number of points in a complex, which were 15 in our example; 3) An evolution step began by randomly selecting and sorting a specified number of points from the complex to create a subcomplex. The probability of a particular point being selected was conditioned by a probability function favoring the best points. By default, the number of points selected was one plus the number of parameters being calibrated. Using all but the worst point in the subcomplex, the average for each parameter was calculated; 4) In this step, iteration was attempted by reflecting each parameter value of the worst subcomplex point through that parameter's average. That created a new sample point. If any of the parameters for the reflected point were outside of their ranges, a "mutated" point was used instead as the new point. A mutation was performed by randomly selecting each parameter value from a gaussian distribution of values using the parameter values from the best point in the subcomplex as the mean and the standard deviation from the entire population of points. If the random selection was outside of that parameter's range, a new selection was made. The objective function value was calculated for the new point. If that value was less than that of the worst point in the subcomplex, the new point replaced the worst point and the evolution step was over. If not, a "contraction" point was created. A contraction point had all of its parameters values halfway between the worst point's parameter values and the average parameter values. If the contraction point's objective function value was better than the worst point's, it replaced the worst point and the evolution step was over. If not, another mutated point was created replacing the worst point whether or not it was better. Either way, the evolution step was now over; 5) The values from subcomplex were put back into the complex and the complex was sorted by increasing objective function value. If more evolution steps needed to be performed, we repeated this from step two; 6) When all evolution steps for a complex were done, the complexes' values were put back into the sample population and the next complex was evolved. Subsequently, the new points were tested for convergence. If they converged or the maximum number of attempts was made or recent attempts were not creating a specified amount of improvement, we stopped calibrating; 7) As another option, reducing the number of complexes, if specified, and repeating from step 1 was possible to use the changed population of points to create a new set of complexes.

In order to represent the basin processes more closely, we delineated them into sub-basins based on the available streamflow gage data. The parameters pertaining to the streamflow were estimated with RMSE and r^2 values and shown in Table 2 with their optimal values estimated through calibration. Among the ten parameters, those that represent the fraction of baseflow, its velocity, the fraction of soil water storage and infiltration appeared to influence the water balance computations. However, the parameters representing the thickness of soil layers and their hydraulic conductivity were also useful to calibrate the model. Table 3 describes the statistics of model performance in other basins once the model was calibrated at White Bird. Additional details on the model performance are described in the Results section.

3.3 Parallelized VIC

In order to facilitate the large scale simulation in the climate change context, a computationally efficient method of hydrologic modeling approach is required. Therefore, a simple but effective method was used to parallelize the VIC algorithms in this study. Upon executing the code, it processed the grid cells and decided which cells were active and needed to be processed, a simple modulus algorithm was used to assign the active grid cells, in a round robin fashion, to however many processes were working together. Other than the initialization and finalization calls to MPI, only two other calls were needed to determine the total number of processes working together (the MPI intercommunicator size), and the process number, called rank, within the group of processes (the rank within the MPI intercommunicator). This method left each copy of the program independent of the others and no communication was performed between them.

In this complex terrain, the snowpack is typically present during the winter in the higher elevations of the headwater region of the basin. In order to demonstrate the declining trends, we chose two locations at the central high mountain area within the Salmon River Basin, the Mill Creek Summit (44°28'N, 114°29'W, 2682 m) and the Morgan Creek (44°51'N, 114°16'W; 2316 m). As the trends in temperature and precipitation are expected to change in the future, it is imperative to expect the implications of these changes in the basin's hydrological processes and subsequent responses in terms of water balance components. Based on the calibrated hydrological parameters and the climate model-derived precipitation and temperature inputs, we simulated the hydrology of the basin to estimate the water balance components, evapotranspiration, runoff, soil moisture and snow water equivalent. Runoff was routed to verify the streamflow at the outlet of the basin, White Bird. Actual evapotranspiration was computed in the model based on the Penman-Monteith formulation which is a function of net radiation and vapor pressure deficit. Canopy evaporation and transpiration from each vegetation portion and bare soil evaporation from the bare soil portion of the grid was used in computing the total actual evapotranspiration, weighted by the fraction of each surface cover type.

4. Results and Discussion

4.1 Historic Analysis (1955-1999)

We analyzed the historic simulated streamflow for multiple locations and in general, the model was able to simulate the streamflow, both in terms of magnitude and timing, at a daily time step. In this study, the sub-basin outlets, namely Clayton, Lemhi, Salmon, Shoup, Yellow Pine, Krassel and Riggins were not individually calibrated and there were some discrepancies either in magnitude or time of peak flows. For this study, however, the behavior of the watershed was characterized by examining the response at the downstream location, White Bird, before the confluence with the Snake River. Since most of the precipitation comes as snow in the basin during the winter, the peak snow melt season can be anywhere between May and July, modulated by temperature trends. Since the simulation period contained both wet and dry water years, the ability of the model to capture the entire range of flows was not only important but required and the range in flows over this long-term period was seen both in the model-simulated and observed streamflow.

Figure 2a shows the calibration and validation of the VIC model using observed streamflows at White Bird. An r^2 value of 0.94 with an RMSE of 103 m^3/s and a similar value of r^2 of 0.94 with an RMSE of 88 m^3/s for the calibration and validation periods, respectively. Overall, the long-term hydroclimatology as the seasonal streamflows, shown in Figure 2b, suggests that the basin outflow peaked in July and low flows persisted between December and February. Typically, the peak flow for any given year was somewhere between 1000 m^3/s and 2000 m^3/s, and low flows were about 100 m^3/s. At least, for about 15 years, the flows peaked at or above 1500 m^3/s, with a peak flow of 2300 m^3/s in July, 1974 and a minimum peak flow of 300 m^3/s in June 1977. As far as the annual average flows were concerned, the outflow from the Salmon River basin at White Bird was between 150-500 m^3/s with an average annual flow of 325 m^3/s. The year 1997 was the highest and 1977 was the lowest in the studied period. Given that both the calibration and validation periods, contained these varied flows and in general, VIC captured these wide ranges of high and low flow annual events. This was considered to be the first crucial step in quantifying the uncertainty in model predictions. Basically, when we performed calibration over 20-years period, the parameters represented in the model captured the average year flow patterns while it missed to capture the extreme high or low years. For instance, wet years in the calibration period, such as 1965 and 1974, the model either over- or

under-estimated in capturing the flow as the average parameters might have missed capturing the peaks to optimize the overall root mean square error for the calibration. Other water budget components from the retrospective analysis showed that partitioning of the water budget was reasonable. The annual total of precipitation of about 800 mm was generally partitioned into 450 mm as evapotranspiration and 350 mm as runoff. Storages in terms of snow water equivalent and soil moisture were also computed as part of the water budget that showed seasonal fluctuation as expected. We verified the snow water equivalent simulated by the model with two Snotel sites (Morgan Creek and Mill Creek) and in general, the model agreed well with a high correlation coefficient of 0.69 and 0.87, respectively.

The performance of the hydrology model was not tested with the historical GCM output, since we used the historical observed dataset to correct the bias in future projections. It may be desirable to understand the GCM characteristics for the study area using historical simulation, however, by comparing the GCM historical downscaled climatology with the observed data, we found the correlation for precipitation was weak. This was probably due to the method that involved random selection of historical observation. The observed dataset was based on point observations of precipitation generated by SYMAP gridding method. This could smooth out the correlation between observed and GCM simulated data. In order to accommodate the uncertainty in GCM products, we therefore choose to use all of the projections in this analysis.

4.2 Climate Model Projected Trends

Based on the CMIP3 projected scenarios, there are 16 models with different emission scenarios resulting in 112 ensembles of projected temperature and temperature. Our analysis of precipitation and temperature change is shown in Figure 3 for different time periods, 2010-40, 2041-70 and 2071-2100 when compared against the long-term historic averages between 1949-1999. Clearly, changes in annual average temperatures were expected to be smaller in the near-term projections, 2010-40, which was about 3 °C warmer than the historic averages. Changes in precipitation was bi-directional, with some models showing increasing precipitation by as much as 15%, and a few other models showing decreasing trends of about 5%, and average of all ensembles showed a 2% increase in precipitation when compared with the historic averages. This is in agreement with the results by Mote and Salathe (2010), Pederson et al. (2010) and Mote (2003) wherein they reported a general increase in precipitation and temperature in this region. However, the uncertainty grew wider in the extended projections for the periods of 2040-70 and 2070-2099 with both precipitation and temperature changes. An average of all ensembles resulted in the increase in precipitation by 5% and 8%, during 2040-70 and 2070-2099, respectively and increase in temperatures were 4 °C and 6 °C for the same period.

Figure 4 shows the long-term season averages of temperature or the sum of precipitation against the future projections. As can be seen from the historic trends, the basin received more precipitation in the form of snow during November through February than any other months of the year. Variability in precipitation on a seasonal scale was quite evident for all the three 30-year projections, 2010-2040, 2040-70 and 2070-2099. Seasonal temperatures, shown in the bottom panel of Figure 4, were as low as -10 °C in the winter and as high as about 15 °C. Future projections of temperatures, on average, showed a warming trend for the same three periods. However, the uncertainty in temperatures was relatively minimal when compared with that of precipitation. A similar trend was reported by Jin and Sridhar (2012) for the Boise and Spokane River basins in Idaho. The ensemble averages showed warming conditions all year around and that was more pronounced in the autumn and spring, between September and March. This is expected to have a significant impact on the basin hydrology and water resources which will be discussed in the following section. On a monthly scale, while the temperature between November and January rose between 1-2 °C when compared with the historical values, an upward magnitude of 2-4 °C was evident in all the three time periods for June and July.

4.3 Altered Hydrological Cycle

Table 4 shows the comparison between the historic and future averages as well as minimum and maximum values for precipitation, temperature, runoff, ET, soil moisture and SWE. As discussed earlier, the model partitioned the majority of the mean annual total precipitation of 800 mm during 1955-1999 between evapotranspiration and runoff, 452 mm and 348 mm, respectively. Seasonal averages of snow water equivalent and soil moisture were about 120 mm and 298 mm, respectively. The ranges in precipitation and ET between historic and future time periods were broad, with historic means were at the lower end of the range in the future. Runoff and SWE future minimum

values were substantially lower than historic averages. Obviously, the annual averages of soil moisture and ranges were not substantially different between the historic and future pattern. Changes to temperature, runoff and ET were statistically significant and soil moisture, SWE and precipitation were not significant.

The emphasis in this study was on capturing the variability and change in the water balance and streamflow and, its direct implications on our ability to demonstrate the climate model projections in relation to basin's hydrology and water management. Because of the increased precipitation and temperature possibilities and a wide range of projections, the other water balance components in the future reflected somewhat of a similar range. By considering the ensemble average, our estimations have shown an increasing evapotranspiration of 5.8 % in 2010-2040, 10% in 2040-2070 and 14% in 2070-2099. However, precipitation increases tend to decrease the runoff potential by about 3-4% until 2070 and increase slightly by less than 1% .With regard to seasonal variability and change, from **Figure 5**, it was evident that early growing season evapotranspiration between April and August was higher than the patterns seen in the hydroclimatology of the basin. Increasing evapotranspiration trends in the future have also been reported for various managed (Vano et al., 2010) and natural river basins in the U.S. West (Jin and Sridhar 2012; Wood et al. 2004;). Runoff variability and change was the highest among the water balance components, with a clear shift in the timing of peak runoff occurring in late spring (May) instead of June or July. Early melt might have resulted in increased soil moisture in the spring and as a result SWE was less than the historical trends. Nevertheless, increased evapotranspiration in the growing season appeared to deplete both SWE and soil moisture between June and September.

4.4 Center of Timing and Snow Water Equivalent

Figure 6 illustrates a comparison of the center of timing (CT) between historical and future trends in streamflows based on all ensembles of climate model outputs that came from A1B, A2 and B1 emission scenarios, covered in the earlier sections. Numerous studies have shown the need for assessing the CT in the western U.S. river basins (Barnett et al. 2005; Sridhar and Nayak 2010), which suggests the timing of streamflow when 50% of annual flows would have occurred in a given water year (Oct-Sep) by a certain day of year (DOY). This also corresponds to the peak of the hydrograph. Historical analysis on the left side of each panel suggests a declining or advancing CT for the period between 1949-1999 with an average CT of 219.2 while the ensemble averages for A1B, A2 and B1 suggests a further advanced CT with 209.2, 208.7 and 211.3, respectively. Also, as shown in Figure 5, we present the uncertainty in the ranges of predicted streamflow and hence in the estimations of CT, when considering all of the ensembles. While it might be widely seen as the uncertainty that might not be helpful for any impact assessment, our intention was to highlight the state of the current generation of climate model outputs and their usefulness in the large basin scale studies such as this. The ranges in CT for A1B was from 166.6 to 240.2, A2 from 159.6 to 241.8 and B1 from 163.3 to 247.3 with lowest numbers referring to warmest and highest numbers to weaker warming climate model projections.

Among the many climate model runs, for the Salmon River basin, based on CT and streamflow analysis, our study suggests that ipsl_cm4, ccsm3_0_3 and ccsm3_0_5 were expecting warmer conditions and mri_cgcm2_3_2a_5, echo_3 and inmcm3_0 were projecting some what cooler conditions in the future. We present the timing of melt and peak flow in Figure 7. Apart from interannual variability seen in both historic and future flows, a gentle slope to the left suggesting an earlier melt appeared to persist in ipsl_cm4, ccsm3_0_3 and ccsm3_0_5-high end warming conditions from A1B, A2 and B1 scenarios. Nonetheless, mri_cgcm2_3_2a_5 and echo_3 appeared to show early melting as well and inmcm3_0 having a high variability in peakflow.

4.5 Declining Snow Water Equivalent Trends

Because the basin receives precipitation mostly as snow which occurs during the winter and spring, we evaluated the future trends in snow water equivalent (SWE) for DJF (December, January and February) in this analysis. In order to remove the effect of interannual variability of total precipitation on the SWE trends, we normalized SWE by precipitation. As there is great variability among the climate models for SWE prediction, an overall ensemble trend of SWE/P for the future model is presented in Figure 8(a-b) for Mill Creek and Morgan Creek. The standard deviation of all the models within each year is also shown as error bars. The plot demonstrated that the SWE/P trends at these two locations could decrease in the future between 2010-2099, however the model variability or uncertainty appeared to increase during the same period.

In order to further study the deviation of future prediction from the historical long-term hydrological condition, we calculated the normalized anomaly of SWE/P as shown in Sridhar and Nayak (2010).

$$\sigma = \frac{SWE/P - \overline{(SWE/P)_{hist}}}{std\ dev[(SWE/P)_{hist}]}$$

However, after scrutinizing all the ensemble members we recognized that some spikes caused by abrupt changes in SWE especially during the transition times of winter to spring and this could potentially bias the trends. Therefore, in order to only compare those years for which SWE increased consistently from December through February, we removed those years that showed phase change during the transition times between February and March.

Figure 9 (a and b) shows that the two locations exhibit similar trends for future SWE/P changes although the distribution for any given year among various models were widely ranging. The normalized anomalies of a majority of GCM scenarios were with decreasing trends except for a few models. The Mill Creek site included 11 scenarios, while the Morgan Creek site contained 9 scenarios. In addition, the ensemble members that showed slopes with an increasing trend were relatively less in number.

In order to filter out the trends, we chose two climate models, ipsl and ccsm3 as the warm and cold models based on our center of timing analysis. Figure 10 shows the maximum decreasing (ipsl) and increasing trend (ccsm3) among the 112 GCM ensembles at the Mill Creek Summit and Morgan Creek. Clearly, the increasing trend was one order of magnitude lesser and the slope was relatively flatter than that of the decreasing trend. Based on the anomaly of SWE/P, the most significantly decreasing model for the Mill Creek Summit was ipsl, A2, for Morgan Creek was ccsm3, A2. The increasing model for the Mill Creek summit was ccsm3, B1 and for Morgan Creek was ccam3, B1. Obviously, B1 scenarios were representing the conservative emission scenarios and in turn demonstrated a weaker warming regimes or wetter precipitation regimes compared to A2 and A1B scenarios that showed decreasing SWE/P and CT. This could imply the decrease of SWE/P might be highly related to warming conditions in the basin and warmer the climate model, lesser the snow accumulated in higher elevations that triggered the decrease in SWE/P.

4.6 Spatial Variability in the Water Budget

We analyzed the spatial patterns in basin scale hydrology and presented in Figure 11. Despite the fact that downscaled precipitation data have shown a wide variability in scenarios, models and decades, temperature rise was consistent for the basin. Using our $1/8^{th}$ degree gridded model output, we aggregated the model output for four seasons, winter, spring, summer and fall for each of the ensemble members and then computed the ensemble averages. This analysis included all of the water balance components, however, we presented only precipitation, runoff, evapotranspiration and soil moisture by computing the difference between future and historic averages in Figure 11. Except the summer, precipitation appeared to increase in the basin, especially in the southwestern corner, by about 10-20 mm and in some areas it exceeded by 30 mm in the winter. This precipitation increase eventually resulted in increased runoff for those areas where increased precipitation was possible, most notably in the spring, as supported by advancing snowmelt from our earlier analysis. Higher elevations were also seen to exhibit decreasing runoff, possibly due to decreased SWE. Summer and fall season runoff were also less by 10-20 mm, especially in the upper basin. This decreased runoff could also be partly explained by the increased evapotranspiration in the spring and summer. Soil moisture was higher than the historical range by about 25-50 mm in the winter and in the southern part of the basin during spring exceeded by 100 mm. This implied that earlier snowmelt and winter rain must have added to the soil moisture storage, and the basin witnessed loss of soil moisture by about 50 mm in the summer and fall and this deficit was further advanced due to increased temperature and summer evapotranspiration. Decrease in soil moisture in this forested basin could be detrimental to the forest and stream health. When there is a reduction in soil moisture, it could trigger drought and wildfire risks. With decreased runoff, when the stream temperature can likely get warmer, it would further inhibit salmon migration for spawning in this basin.

5. Conclusions

Climate change is expected to show unforeseen impacts in the Pacific Northwest and in order to prepare the planning or adaptation techniques sound science is necessary. In this study, we evaluated the hydrologic impacts for a relatively remote but ecologically important basin, SRB, located in central Idaho. Among the hydrological indicators, streamflow and the water balance components were focused in our analysis. In general, the climate model ranges in precipitation and temperature showed a wide margin, however, a consistently increasing pattern was seen in the study basin, SRB. Comparisons of the climate model ensembles from A1B, A2 and B1 scenarios, for the three periods, 2010-2040, 2040-70 and 2070-99 with the historical trends averaged over 1949-99, highlighted an increase of 3.1 °C, 4.2 °C and 5.3 °C while the precipitation trends were up by 1.8, 4.6 and 8% over the same period.

As these trends were expected to have significant hydrological impacts, we investigated the response of the basin to these probable changes in the future. We demonstrated the improved macroscale hydrological model, VIC, by linking the climate model forcings to evaluate the basin hydrology. Clearly, on average the snowmelt-induced peakflows were advancing by 10 days from our center of timing analysis when compared with historical periods. The ensemble average of center of timing showed a steep decline for the next 90 years with A2 being the highest. Depletion of SWE and soil moisture just after the peak snowmelt into the growing season appeared to be considerable and this could directly have implications for drought, wildfire risks and low flows. This in turn can impact the stream temperature and salmon migration and spawning. Hence, the consequences of climate change for SRB can be significant. One interesting question to ask by looking at this vast range of predictions is how does it impact our management of water resources? It may not be easy to rule out one model predictions against the other, rather a more guided approach could prove the consistency in altered flow regimes and the resulting advancement of CT among all model scenarios could be construed as consistent enough in reassuring the impacts to develop policies and plans. High resolution modeling as well as multi-model analysis to characterize the uncertainty in streamflow and water balance at the sub-basin scale is required and that will provide further insights into the heterogeneous characteristics of this basin in a warming world.

Acknowledgements

This research is supported by the NSF Idaho EPSCoR Program and by the National Science Foundation under award number EPS-0814387. Partial support came from NOAA via the Pacific Northwest Climate Impacts Research Consortium under award number NA10OAR4310218.

References

Abatzoglou, J (2011) Influence of the PNA on declining mountain snowpack in the Western United States, International Journal of Climatology, 31: 1135-1142.

Adbulla F.A., Lettenmaier DP (1997) Application of regional parameter estimation schemes to simulate the water balance of a large continental river. Journal of Hydrology, 197, 258-285.

Adam JC, Hamlet AF, Lettenmaier DP (2009) Implications of global climate change for snowmelt hydrology in the 21st century. Hydrological Processes, 23(7), 962-972.

Barnett TP, Adam JC, Lettenmaier DP (2005) Potential impacts of a warming climate on water availability in snow-dominated regions. Nature, Vol. 438, doi: 10.1038/nature04141, 17 November 2005.

Cherkauer K A, Lettenmaier DP (2003) Simulation of spatial variability in snow and frozen soil Field. J. Geophy. Res.,Vol. 108, No. D22, 8858-, doi:10.1029/2003JD003575.

Cuo L, Beyene TK, Voisin N, Su F, Lettenmaier DP, Alberti M, Richey JE (2011) Effects of mid-twenty-first century climate and land cover change on hydrology of Puget Sound basin, Washington, Hydrological Process, 25: 1729-1753.

Daly C, Neilson RP, Phillips, DL (1994) A statistical–topographic model for mapping climatological precipitation over mountainous terrain, J. Appl. Meteor., 33, 140–158.

Daly C, Taylor GH, Gibson, WP (1997) The PRISM approach to mapping precipitation and temperature, Preprints, 10th Conf. on Applied Climatology, Reno, NV, Amer. Meteor. Soc., 10–12.

Duan Q, Gupta VK, Sorooshian S (1993) A shuffled complex evolution approach for effective and efficient global minimization. J. Optim. Theory Appl., 76, 501–521.

Fowler HJ, Blenkinsop S, Tebaldi C (2007) Linking climate change modeling to impact studies: recent advances in downscaling techniques for hydrological modeling. Intl Journal of Climatology, 27, 1547-1578, DOI: 10.1002/joc.1556.

Graham LP, Hagemann S, Jaun S, Beniston M (2007a) On interpreting hydrologic change from regional climate models. Climatic Change, 81, 97-122, DOI 10.1007/s10584-006-9217-0.

Graham LP, Andreasson J, Carlsson B (2007b) Assessing climate change impacts on hydrology from an ensemble of regional climate models, model scales and linking methods- a case study on the Lule River Basin. Climatic Change, 81, 293-307.

Hamlet AF, Mote PW, Clark MP, Lettenmaier DP (2007) 20th Century Trends in Runoff, Evapotranspiration, and Soil Moisture in the Western U.S.. J. Climate, 20 (8): 1468-1486.

Hamlet AF (2011) Assessing water resources adaptive capacity to climate change impacts in the Pacific Northwest Region of North America, Hydrol. Earth Syst. Sci., 15: 1427-1443.

Hoekema D ., Sridhar V (2011) Relating climatic attributes and water resources allocation: A study using surface water supply and soil moisture indices in the Snake River basin, Idaho. Water Resources Research, doi:10.1029/2010WR009697, 47, W07536, doi:10.1029/2010WR009697.

Jin X, Sridhar V (2012) Impacts of climate change on hydrology and water resources in the Boise and Spokane River Basins. Journal of American Water Resources Association, (in press)

Jung, IW. and Chang, H. (2011a), Climate change impacts on spatial patterns in drought risk in the Willamette River Basin, Oregon, USA, Theoretical and Applied Climatology doi:10.1007/s00704-011-0531-8.

Jung IW, Chang H (2011b) Assessment of future runoff trends under multiple climate change scenarios in the Willamette River Basin, Oregon, USA, Hydrological Process, 25: 258-277

Jung IW, Chang H, Moradkhani H (2011) Quantifying uncertainty in urban flooding analysis considering hydro-climatic projection and urban development effects, Hydrol. Earth Syst. Sci., 15: 617-633

Kalnay E., and Coauthors (1996) The NCEP/NCAR 40-Year Reanalysis Project, Bull. Amer. Meteor. Soc., 77, 437–471.

Kerr RA (2011) Vital details of global warming are eluding forecasters. Science, 334, 173-174, 14 October 2011.

Kimball, JS, Running, SW, Nemani, R (1997) An improved method for estimating surface humidity from daily minimum temperature, Agric. For. Meteor., 85, 87–98.

Liang X, Lettenmaier DP, Wood EF, Burges SJ (1994) A simple hydrologically based model of land surface water and energy fluxes for general circulation models. J. Geophys. Res., 99(D7), 14,415-14,428, July 1994.

Liang X, Wood EF, Lettenmaier DP (1996) Surface soil moisture parameterization of the VIC-2L model: Evaluation and modifications. Global and Planetary Change, 13(1-4), 195-206, June 1996.

Matter MA, Garcia LA, Fontane DG, Bledose B (2010) Characterizing hydroclimatic variability in tributaries of the Upper Colorado River Basin-WY1911-2001. Journal of Hydrology, 380, 260-276.

Maurer EP, Wood AW, Adam JC, Lettenmaier DP, Nijssen B (2002) A long-term hydrologically based dataset of land surface fluxes and states for the conterminous United States. Journal of Climate, 15, 3237-3251.

Milly PCD, Betancourt J, Falkenmark M, Hirsch RM, Kundzewicz ZW, Lettenmaier DP, Stouffer RJ (2008) Stationarity is dead: Whither water management. *Science* 319, 573-574.

Minshall GW, Peterson RC, Bott TL, Cushing CE, Cummins KW, Vannote RL, Sedell JR (1992) Stream Ecosystem Dynamics of the Salmon River, An 8th-Order System. Journal of the North American Benthological Society, Vol. 11, No. 2, 111-137.

Mote PW (2003) Trends in temperature and precipitation in the Pacific Northwest during the twentieth century. Northwest Science, 77(4), 271-282.

Mote, P., and E. Salathé. (2010) Future climate in the Pacific Northwest." Climatic Change, 102(1-2), 29-50.

Nijssen B, Lettenmaier DP, Liang X, Wetzel SW, Wood EF (1997) Streamflow simulation for continental-scale river basins. Water Resour. Res., 33, 711-724.

Olesen JE, and 15 authors (2007) Uncertainties in projected impacts of climate change on European agriculture and terrestrial ecosystems based on scenarios from regional climate models. Climatic Change, 81, 123-143.

Pederson GT, Graumlich LJ, Fagre DB, Kipfer T, Muhlfeld CC (2010) A century of climate and ecosystem change in Western Montane: what do temperatures portend? Climatic Change, 98, 133-154, DOI 10.1007/s10584-009-9642-y.

Shepard DS (1984) Computer mapping: The SYMAP interpolation algorithm. Spatial Statistics and Models, G. L. Gaile and C. J. Willmott, Eds., D. Reidel, 133–145.

Shi X, Wood AW, Lettenmaier DP (2008) How essential is hydrologic model calibration to seasonal streamflow forecasting?. Journal of Hydrometeorology, 9, 1350-1362, DOI: 10.1175/2008JHM1001.1

Shukla S, Steinemann AC, Lettenmaier DP (2011) Drought monitoring for Washington State: indicator and applications, Journal of Hydrometeorology, 12: 66-83.

Sridhar V, Nayak A (2010) Implications of climate-driven variability and trends for the hydrologic assessment of the Reynolds Creek Experimental Watershed, Idaho. Journal of Hydrology, 385, doi:10.1016/j.jhydrol.2010.02.020, 183-202.

Thornton PE, Running, SW (1999) An improved algorithm for estimating incident daily solar radiation from measurements of temperature, humidity, and precipitation, Agric. For. Meteor., 93, 211–228.

Vano JA, Scott M, Voisin N, Stöckle CO, Halmet AF, Mickleson KEB, Elsner MM, Lettenmaier DP (2010) Climate change impacts on water management and irrigated agriculture in the Yakima River basin, Washington, USA. Climatic Change, Vol. 102, Issue 1-2, 287-317, doi:10.1007/s10584-010-9856-z

Voisin N, Schaake JC, Lettenmaier DP (2010) Calibration and downscaling methods for quantitative ensemble precipitation forecasts. Weather And Forecasting, 25 (6), pp 1603-1627.

Wood AW, Leung LR, Sridhar V, Lettenmaier DP (2004) Hydrologic implications of dynamical and statistical approaches to downscaling climate model outputs. Climatic Change Vol. 62, Issue 1-3, 189-216.

List of Tables

Table 1. Climate models employed in the hydrological impact assessment study. These are based on the IPCC Special Report on Emission Scenarios (SRES). The emission scenarios are A2 (high end and no stabilization), B1 (low end with 550 ppm) and A1B (intermediate case with 750 ppm).

Modeling Center	Country	Model	SRES simulations
Bjerknes Centre for Climate Research	Norway	bccr-bcm2.0	A1B, A2, B1
Canadian Centre for Climate Modeling & Analysis	Canada	cccma cgcm3.1 (t47)	A1B, A2, B1
Centre National de Recherches Meteorologiques Coupled global climate Model	France	cnrm-cm3	A1B, A2, B1
Climate System Model, CSIRO Atmospheric Research	Australia	csiro-mk3.0	A1B, A2, B1
US Dept. of Commerce / NOAA / Geophysical Fluid Dynamics Laboratory	USA	gfdl-cm2.0	A1B, A2, B1
US Dept. of Commerce / NOAA / Geophysical Fluid Dynamics Laboratory	USA	gfdl-cm2.1	A1B, A2, B1
Goddard Institute for Space Studies, NASA	USA	giss-er	A1B, A2, B1
Institute for Numerical Mathematics	Russia	inm-cm3.0	A1B, A2, B1
Institut Pierre Simon Laplace	France	ipsl-cm4	A1B, A2, B1
Center for Climate System Research, National Institute for Environmental Studies, and Frontier Research Center for Global Change (JAMSTEC)	Japan	miroc3.2 (medres)	A1B, A2, B1
Meteorological Institute of the University of Bonn (MIUB), Meteorological Research Institute of KMA (METRI), and Model and Data group (M&D)	Germany & Korea	echo-g	A1B, A2, B1
Max Planck Institute for Meteorology	Germany	echam5/ mpi-om	A1B, A2, B1
Meteorological Research Institute	Japan	mri-cgcm2.3.2	A1B, A2, B1
National Center for Atmospheric Research	USA	ccsm3	A1B, A2, B1
National Center for Atmospheric Research	USA	pcm	A1B, A2, B1
Hadley Centre for Climate Prediction and Research/Met Office	United Kingdom	ukmo-hadcm3	A1B, A2, B1

Table 2. Various VIC parameters used in the calibration of the Salmon River at White Bird, Idaho.

Parameters	**Description**	**calibration range**	**optimal value**
Ds	Fraction of Dsmax where non-linear baseflow begins (%)	0-1	0.8199
Dsmax	Maximum velocity of basef (mm/day)	0-30	0.5704
Ws	Fraction of maximum soil moisture where non-linear baseflow occurs (%)	0-1	0.4242
binf	Variable infiltration curve parameter	0-0.4	0.2412
Hs1	Thickness of soil layer 1 (m)	0.1-1.5	0.2629
Hs2	Thickness of soil layer 2 (m)	0.1-1.5	0.5122
Hs3	Thickness of soil layer 3 (m)	0.1-1.6	0.5867
Ksat,1	Saturated hydraulic conductivity of soil layer 1(mm/day)	0-9999	2427.5
Ksat,2	Saturated hydraulic conductivity of soil layer 2 (mm/day)	0-10000	6085.74
Snow Roughness	Surface roughness of snowpack (m)	0.0005 - 0.05	0.0155

Table 3. Model performance at the sub-basin outlets based on monthly flows.

Sub-basins	r^2	RMSE (m^3/s)
Clayton	0.76	29
Salmon	0.66	45
Shoup	0.70	44
Yellow Pine	0.75	20

Table 4. Comparisons of the water balance between future projections and historical averages over the multi-decadal time periods.

Year	Precipitation (mm)			Temperature (°C)			ET (mm)			Runoff (mm)		
	annual total			annual mean			annual total			annual total		
	mean	max	min	mean	max	min	mean	max	min	mean	max	min
1955-2000	799.7	1073.0	572.3	1.9	2.9	0.3	452.3	515.1	401.7	347.6	409.8	59.3
2010-2040	813.8	953.6	720.4	3.1	4.1	2.3	478.8	513.1	452.3	334.9	431.6	261.8
2040-2070	836.5	1040.7	724.5	4.2	5.5	2.7	498.3	551.1	457.7	338.5	496.0	248.4
2070-2099	863.9	1096.4	706.9	5.3	7.6	3.6	515.1	591.1	461.7	348.9	509.7	242.9

Year	SWE (mm)			Soil moisture (mm)		
	annual avg			annual avg		
	mean	max	min	mean	max	min
1955-2000	120.2	216.6	35.3	298.8	370.4	225.5
2010-2040	106.9	137.2	78.0	291.5	333.3	255.0
2040-2070	98.2	123.6	73.5	292.1	370.5	254.4
2070-2099	87.9	149.8	49.7	297.1	365.3	247.7

List of Figures

Figure 1. Location Map showing the Salmon River Basin (SRB) in Southcentral Idaho.

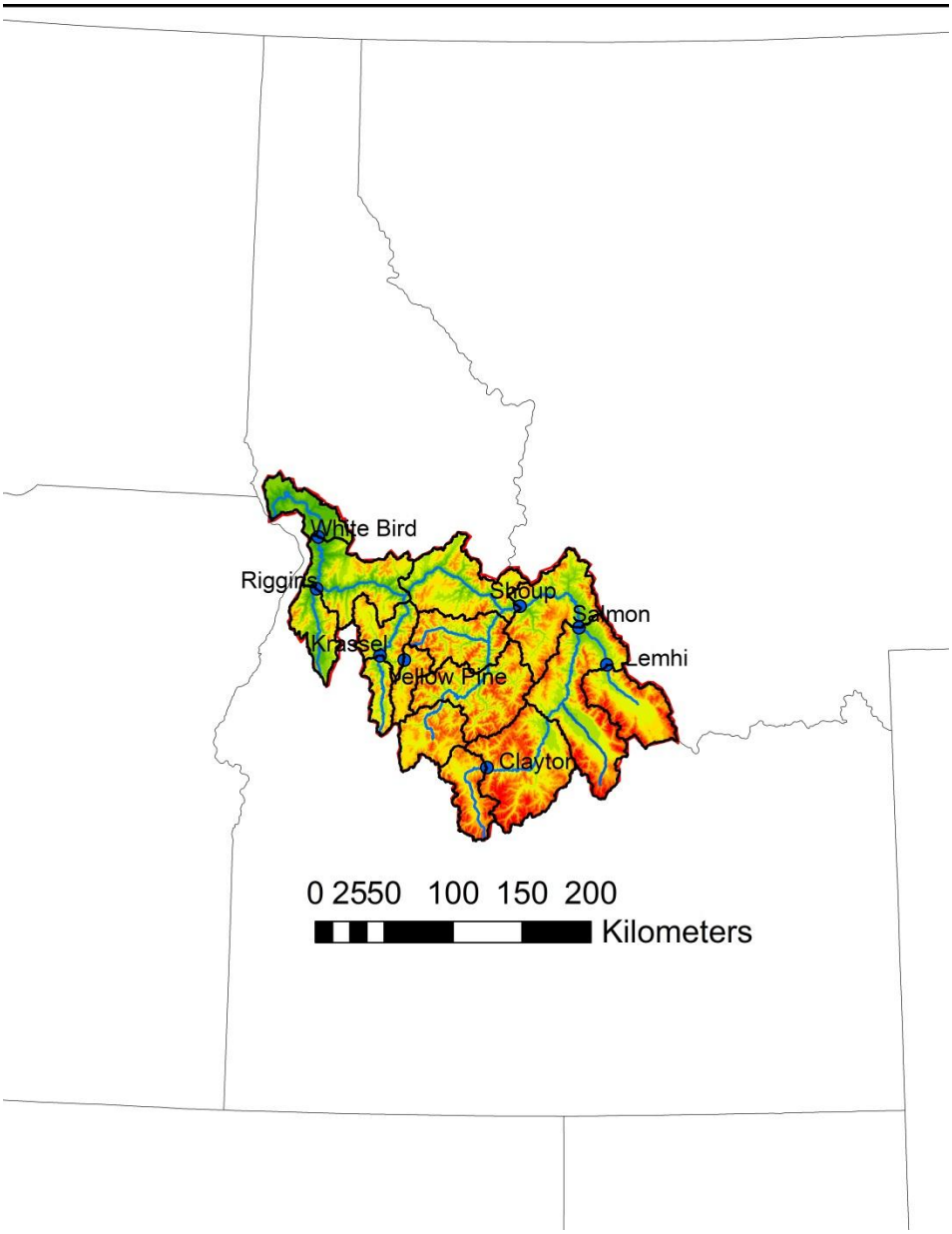

Figure 2. Time series of streamflow at White Bird, Idaho for (a) calibration (b) validation of Variable Infiltration Capacity (VIC) hydrology model.

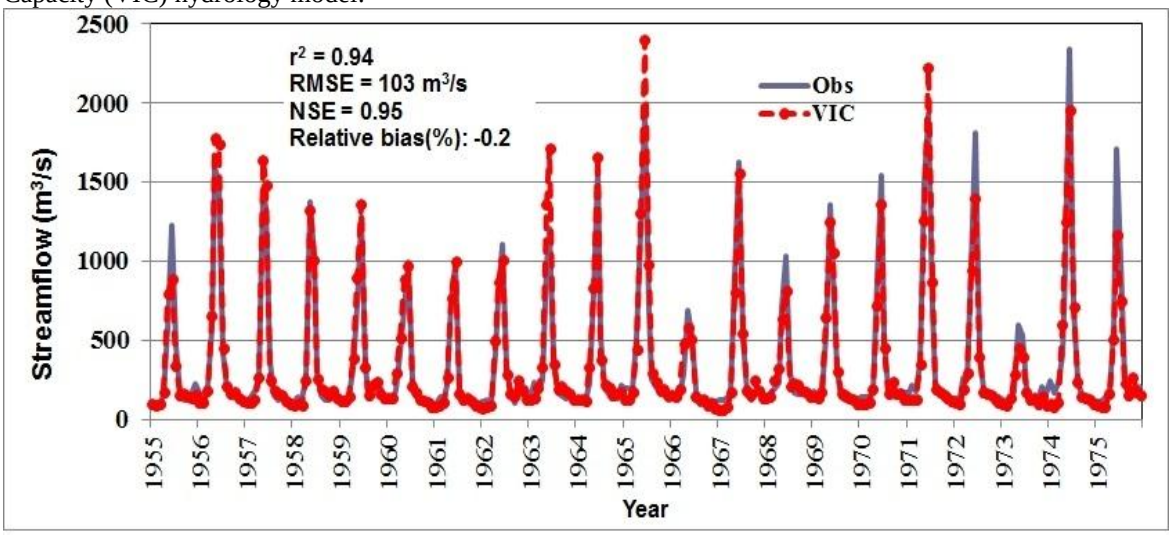

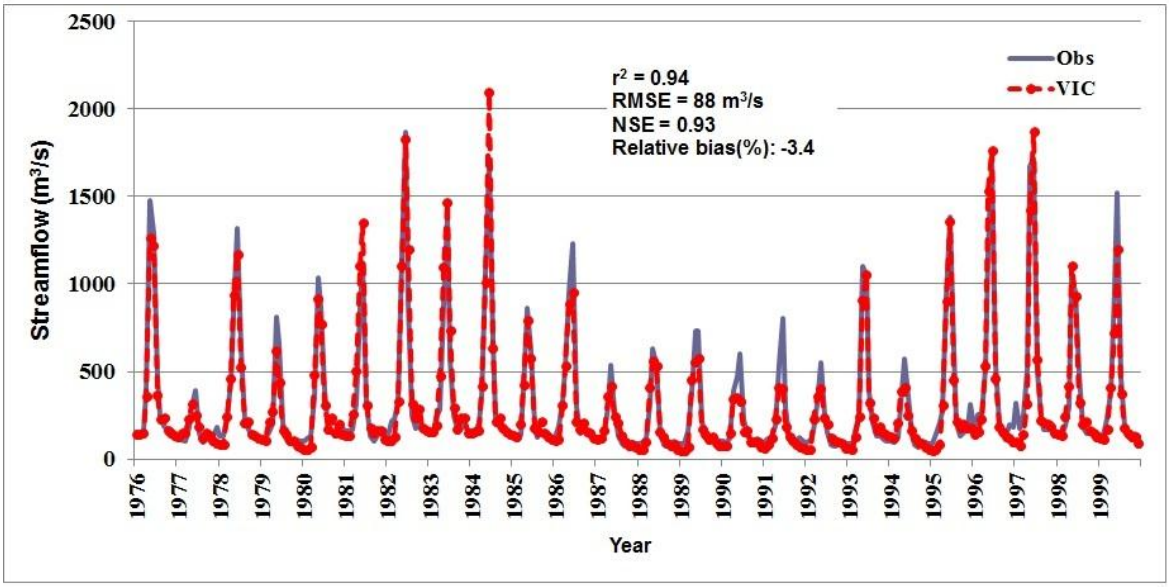

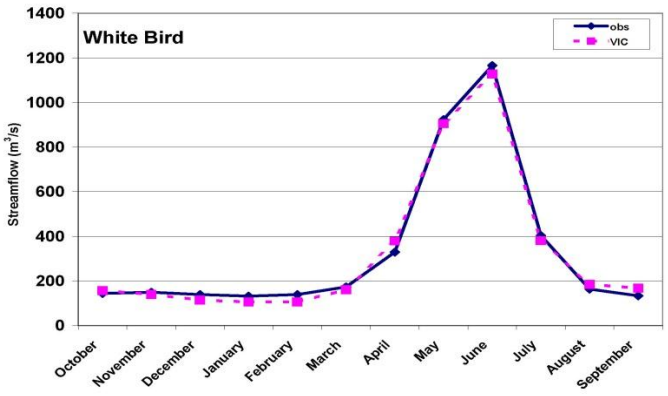

Figure 3. Changes in temperature and precipitation as projected by 16 Global Circulation Models (GCMs) for A1B, A2 and B1 scenarios during the three 30-year time domains, 2010-2040, 2040-70 and 2070-2099.

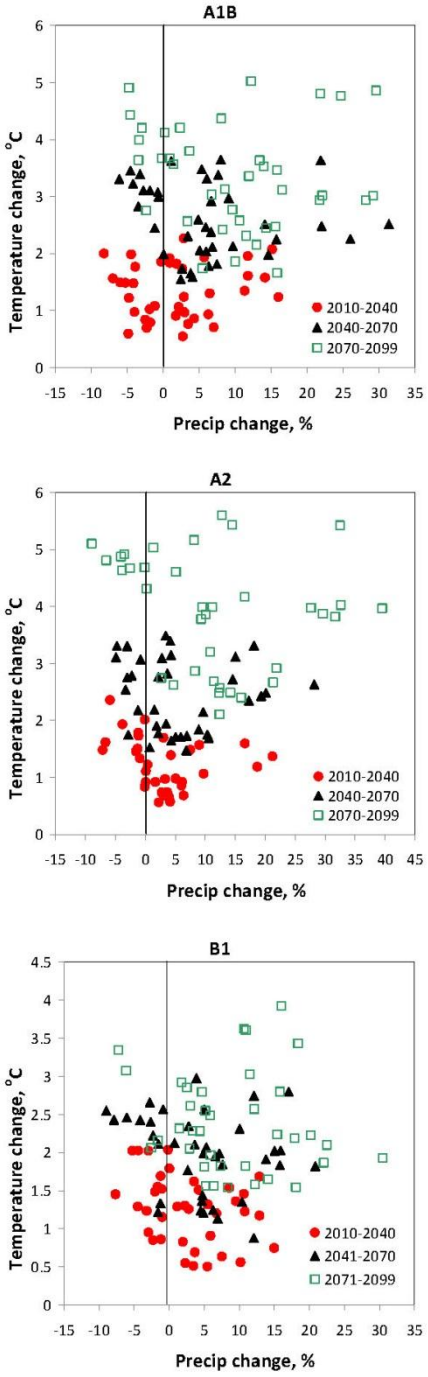

Figure 3

Figure 4. Seasonal projections of precipitation and temperature with all ensemble members (112) and average of all ensembles for the three 30-year time domains, 2010-2040, 2040-70 and 2070-2099.

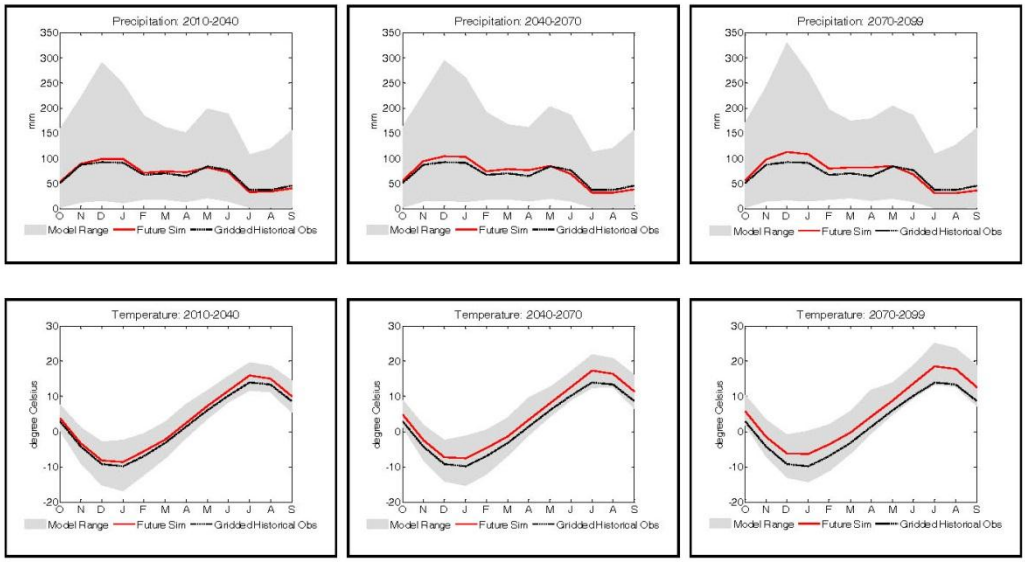

Figure 4

Figure 5. Simulated water balance components from all ensemble members of evapotranspiration, snow water equivalent, runoff and soil moisture for the three 30-year time domains, 2010-2040, 2040-70 and 2070-2099.

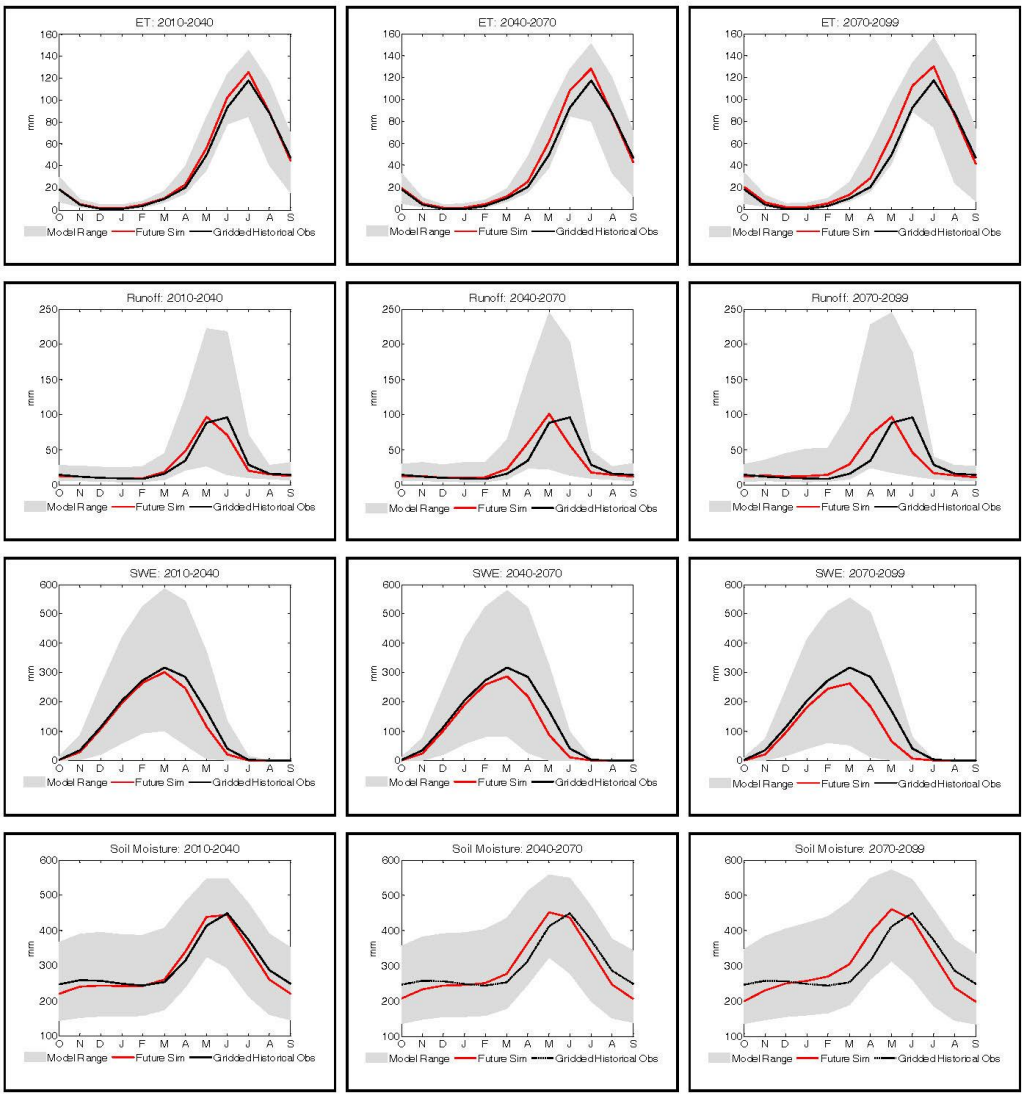

Figure 5

Figure 6. Center of timing for each emission scenarios (a) A1B (b) A2 and (c) B1 showing the gradual decline (or advancement of snowmelt) when compared with historical trends at White Bird, Idaho

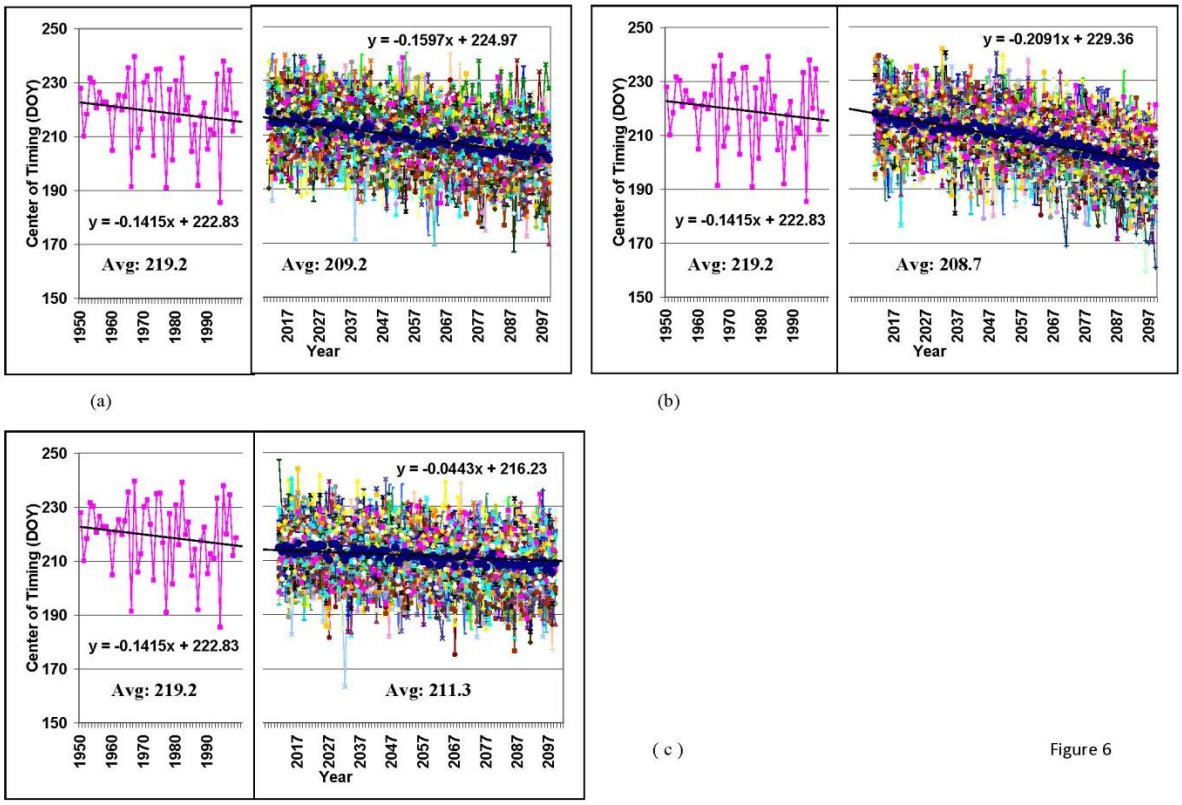

Figure 6

Figure 7. Daily streamflows shown as time maps for 6 different climate models (a) ipsl, A1B (b) ccsm, A2, 3 (c) ccsm, B1, 5 (d) mri, A1B, 5 (e) echo, A2, 3 (f) inmcm, B1 and compared against observed and model-simulated sreamflow for the historic climate.

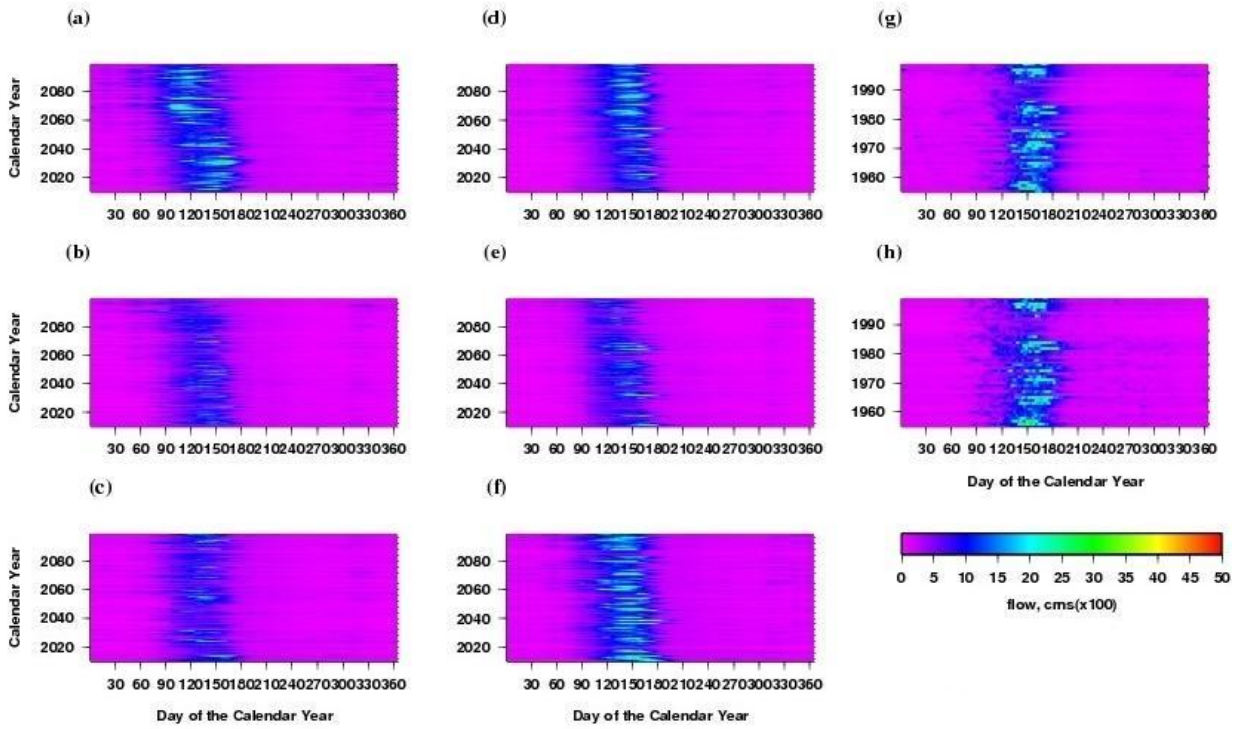

Figure 8. Time series of anticipated SWE/P declining trends computed as the ensemble average during the period between 2010-2099 for (a) Mill Creek Summit and (b) Morgan Creek, two high elevation sites in the Salmon River Basin.

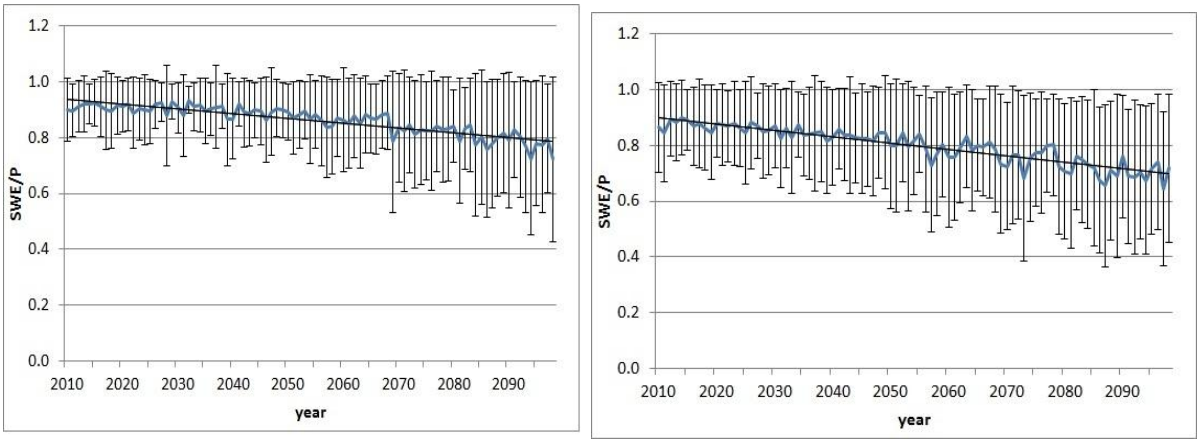

Figure 9. Slope of regression line computed from the normalized anamoly for the SWE/P at (a) Mill Creek Summit (b) Morgan Creek. Out of 112 GCM scenarios, a vast majority of the ensemble members showed a decreasing slope.

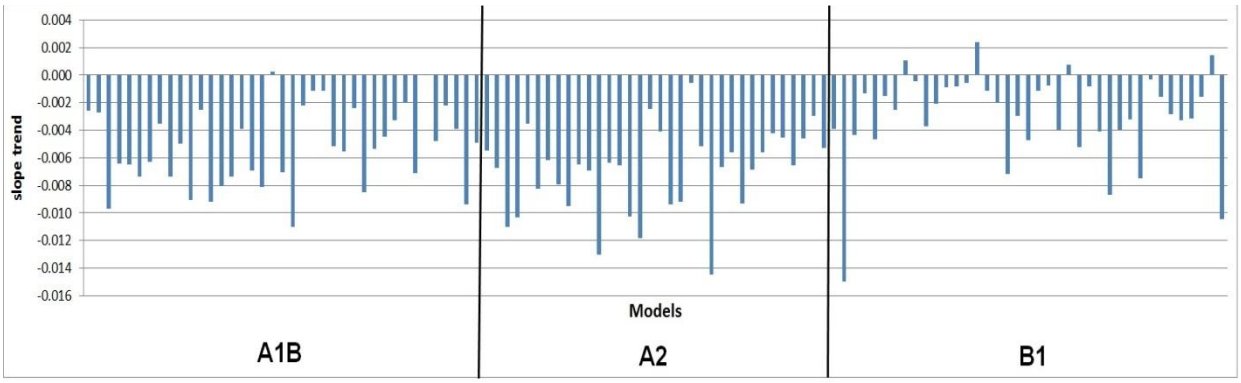

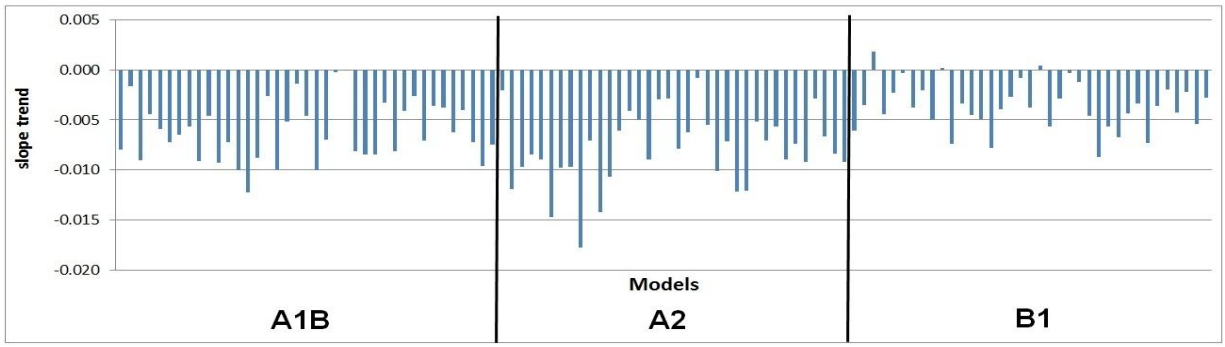

Figure 10. Trends in anomaly from two climate model extremes (a) maximum SWE decrease at Mill (ipsl, A2, run 1) (b) maximum SWE increase Mill (ccsm3, B1, run 7) (c) maximum SWE decrease at Morgan (ccsm3, A2, run 3) (d) maximum SWE increase at Morgan (cccma, B1, run 2)

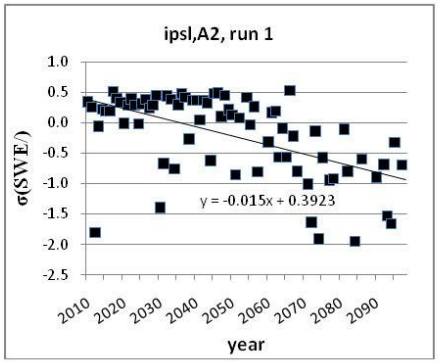

(a)

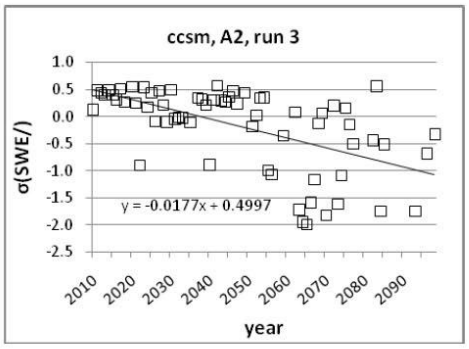

(b)

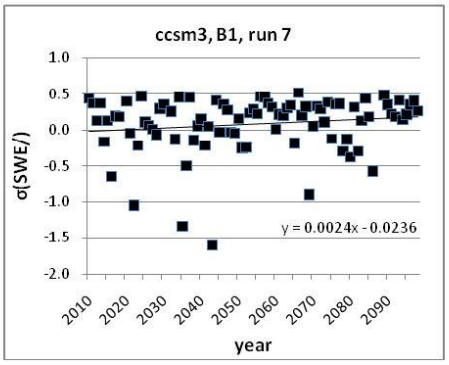

(c)

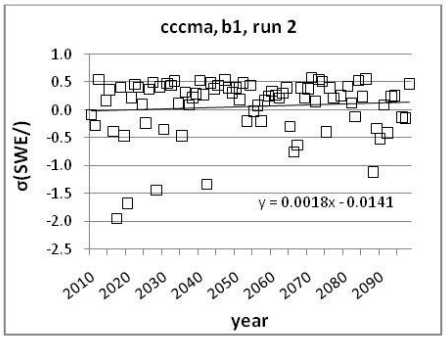

(d)

Figure 10

Figure 11. Differences between future ensemble averages (2010-2099) to historic averages (1949-99) for (a) precipitation (b) runoff (C) evapotranspiration and (d) soil moisture

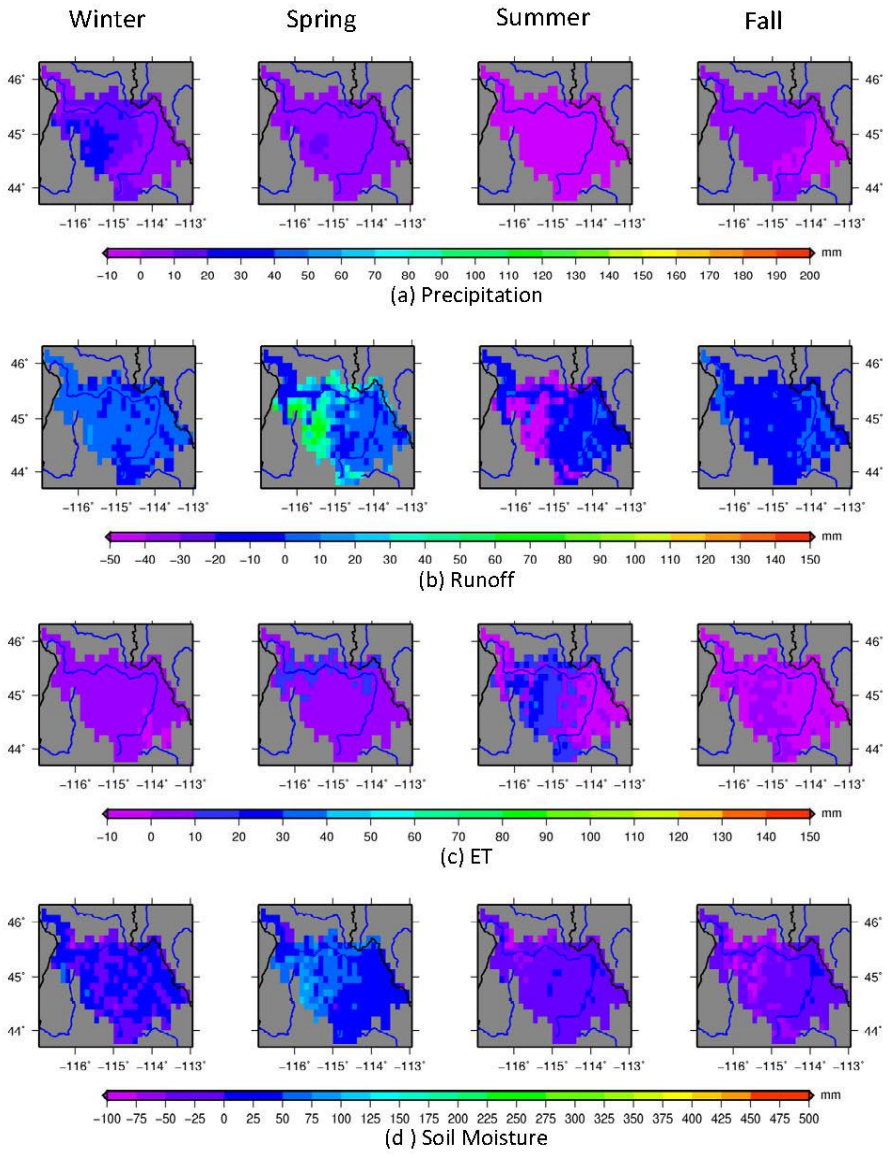

Figure 11